

Synthesis and characterization of G-C₃N₄ @ ZnO photo catalyst on removal of toxic pollutants

S. Kalaiarasan^{a,*}, C. Shanthi^b

^a*Department of Chemistry, Sona College of Technology, Salem.636005, Tamilnadu, India*

^b*Department of Physics, Sona College of Technology, Salem.636005, Tamilnadu, India*

g-C₃N₄@ZnO, pristine ZnO, g-C₃N₄ nanocomposites were synthesized by one-pot hydrothermal approach using urea, zinc nitrate hexahydrate, and hexamethylenetetramine as constituents. X-ray diffraction, scanning electron microscope, diffuse reflectance spectroscopy were used to characterize the g-C₃N₄@ZnO nanocomposites. The photocatalytic efficiency of g-C₃N₄@ZnO, pristine ZnO, g-C₃N₄ nanocomposites was tested using a nitrophenol decomposition test under solar light illumination. The photocatalytic performance of g-C₃N₄@ZnO nanocomposites was higher than that of pure ZnO and elevated with the g-C₃N₄ material. Whenever the g-C₃N₄ content was the photocatalytic activity reached its peak efficiency of 97.8 percent. Moreover, the ZnO/g-C₃N₄ photocatalyst could be reused several times without appreciable loss of activity, showing great potential to be an excellent candidate for environmental remediation.

(Received November 29, 2021; Accepted April 4, 2022)

Keywords: g-C₃N₄, ZnO, Hydrothermal, nitrophenol dye, Visible light

1. Introduction

Economic crisis in latest generations have led to severe ecological issues due to the unregulated release of hazardous contaminants into water and the atmosphere. Developing cost-effective and obvious solutions for eliminating dangerous pollutants has recently received a lot of attention [1–3]. Photo catalysis is a potential technology for treating wastewater even though it is environmentally and cost-effective, and it can degrade a wide range of organic dyes or contaminants. Zinc oxide (ZnO) is a metal oxide semiconductor that has a relatively large energy band gap (3.2 eV), good mechanical, heat transfer, and chemical durability, is harmless, and is cheap [4-6] ZnO is widely regarded as one of the most interesting photocatalysts substances. ZnO, on the other hand, has a reduced photocatalytic performance in visible region compared to UV light owing to its wide band gap. Furthermore, the trickle charger transport splitting in ZnO limits its practicability [7-9] Numerous attempts have been developed to achieve better the photocatalytic performance of ZnO-based photo - catalysts by doping or compositing with metals, nonmetallic, carbon-based composites (graphene, graphene oxide, and reduced graphene oxide) [10, 11] or entanglement with recognisable energy band gap semiconductor to establish Z-scheme [12, 13] Nevertheless, work on a more effective ZnO-based photo - catalyst with higher photocatalytic efficacy is still ongoing. Graphitic carbon nitride (g-C₃N₄) is a stabilizing, metal-free, p-conjugative, and n-type polymers semiconducting with a low energy band gap (2.7 eV). That could be a promising viewable photocatalysts composites associate for ZnO. Because the two substances possess well, intersecting binding energy, combining ZnO with g-C₃N₄ should result in an outstanding heterojunction for improving charge separation. These heterostructures have been found to boost photocatalytic activity in earlier studies. The enhancement is described by the movement of a noticeable electrons from the g-conduction C₃N₄ band (CB) to the CB of the g-conduction C₃N₄'s group (CB) of the g-C₃N₄ to the CB of ZnO [14, 15]. The goal of the proposed is to use the one-pot hydrothermal approach to built and characterization of g-C₃N₄@ZnO

* Corresponding author: kalaiarasans@sonatech.ac.in
<https://doi.org/10.15251/JOR.2022.182.219>

nanocomposites at constant temperature. X-ray diffraction, diffuse reflectance spectra, and scanning electron microscopy examination were used to analyze the impact of g-C₃N₄ concentration on the microstructural, optical characteristics, and photocatalytic activities of g-C₃N₄@ZnO. The decomposition of nitrophenol dye under visible light illumination was used to assess photo catalytic activity. Nanocomposite reusability was also investigated. Particularly photo degradation behavior of g-C₃N₄@ZnO was addressed.

2. Samples preparation

All synthetic substances were of insightful grade and were utilized with next to no further sanitization. Graphitic carbon nitride (g-C₃N₄) was blended by pyrolyzing urea in a mute heater at 520°C for 2h. In the wake of chilling off continuously to room temperature (RT), the toughened sample was ground by an agate mortar to acquire the g-C₃N₄ powder in light yellow tone for additional utilization. Nanocomposites of zinc oxide and graphitic carbon nitride were combined by the one-venture aqueous strategy by means of the accompanying system: dissolving 1.485 g Zn(NO₃)₂·6H₂O into 50 ml refined water, dissolving 0.700 g HMTA into 50 mL refined water, blending two arrangements in with the [HMTA]/[Zn²⁺] volume proportion of 1 : 1 under mixing for 10 mins at RT, and adding g-C₃N₄ into these arrangements. The subsequent blend was moved to an autoclave for the aqueous course at 90°C for 6 h. The items were gathered and washed twice with outright ethanol and refined water and afterward dried in the stove at 80°C for 24 h. At last, a fine white to dim powder was acquired [16].

2.1. Photocatalysis examination

The photocatalytic efficiencies of the g-C₃N₄@ZnO nanocomposites and perfect ZnO were assessed through O-nitrophenol color corruption explore at room temperature. Normally, 50 mg of the photocatalyst was scattered in 100 mL O-nitrophenol watery arrangement (10 mg/L). The above blend was mixed in dull for 60 min to accomplish an adsorption-desorption harmony. The blend was then enlightened under apparent light utilizing a 250 W Osram light outfitted with a 420 nm remove channel at room temperature. A combination of 5 mL arrangement was tested at every 15-minute stretch and afterward was centrifuged to eliminate the photocatalyst solids at 7000 rpm for 10 mins. The UV-Vis ingestion spectra of the subsequent supernatant were estimated by a Cary 100 spectrophotometer (VARIAN) to decide the nitrophenol focus.

3. Results and discussion

3.1. Structural and crystal phase analysis

The XRD samples of g-C₃N₄, ZnO and ZnO/g-C₃N₄ composite displayed in Fig. 1(A). The XRD example of g-C₃N₄ showed a top at 27.6⁰, compares to the (002) plane. It addresses the between planar stacking of sweet-smelling frameworks present in the example with an interlayer distance of 0.326 nm [17]. The as-arranged ZnO additionally showed profoundly exceptional diffraction tops at the 2θ upsides of 31.8⁰, 34.3⁰, 36.5⁰, 47.3⁰, 56.5⁰ and 62.8⁰. These pinnacles were identified with the arrangement of hexagonal wurtzite translucent injury of ZnO [18] not withstanding these pinnacles, the trademark pinnacle of g-C₃N₄ at 27.6⁰ was likewise found in the ZnO/g-C₃N₄ composite which uncovered that the development composite. In addition, the crystalline of ZnO was fundamentally decreased after the consolidation of g-C₃N₄. The shortfall of other diffraction tops in the XRD designs demonstrates that no polluted gem stages and mixtures were framed in the sample.

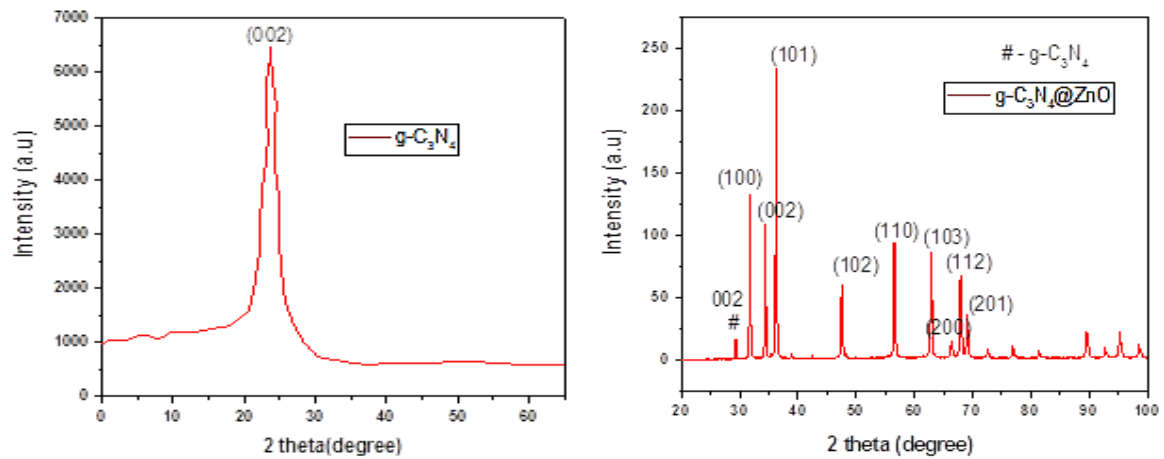


Fig. 1. Powder X-ray diffraction pattern of $g\text{-C}_3\text{N}_4$ and $g\text{-C}_3\text{N}_4\text{@ZnO}$ nanocomposites.

3.2. SEM analysis

The surface morphology and compound piece of the as prepared tests were researched utilizing field outflow examining electron microscopy (FESEM) and energy-dispersive X-beam spectroscopy (EDX), individually and the outcomes were introduced in Fig. 3.

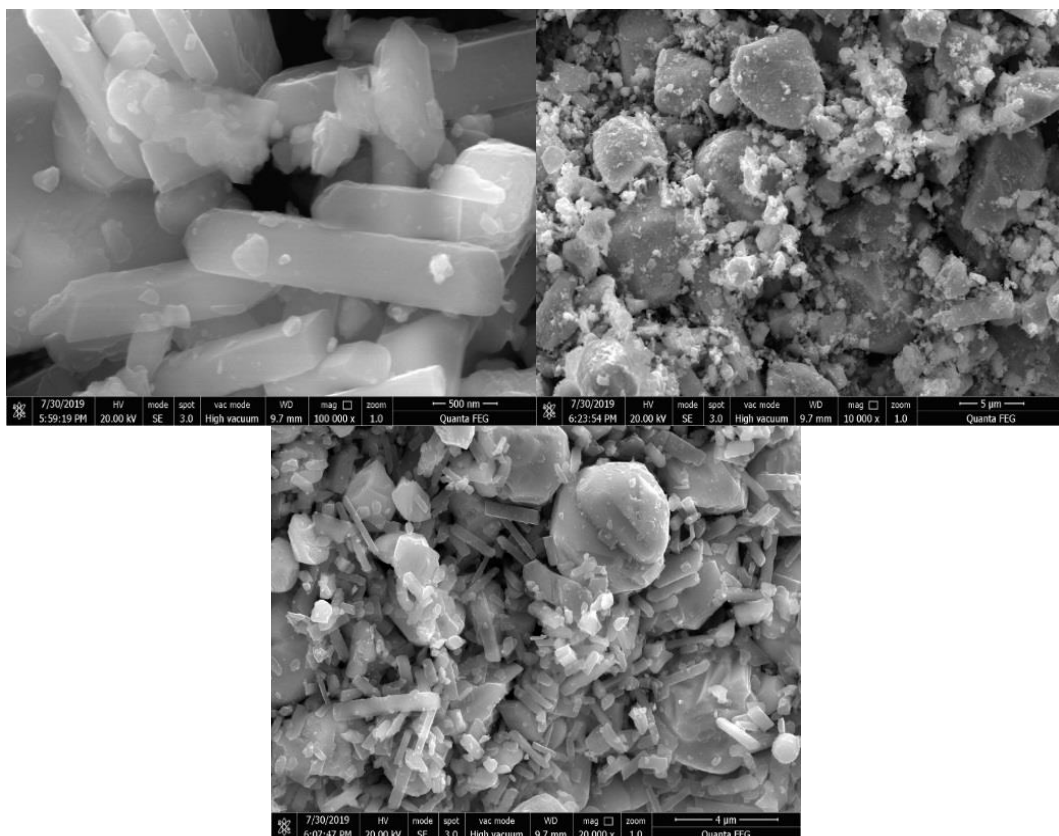


Fig. 2 Morphological spectrum of (a) ZnO, (b) $g\text{-C}_3\text{N}_4$ and (c) $g\text{-C}_3\text{N}_4\text{@ZnO}$ nanocomposites

As displayed in Fig. 3(a and b), the rod and dumble like ZnO microstructures were seen with uniform size conveyance. The length of the Djembe like ZnO structures was estimated to be in micrometer scales. Fig. 3 (b) shows the presence of Zn and O as components in the EDX range.

It further affirmed the arrangement of ZnO without sullied components. Fig. 2 shows the FESEM pictures of the ZnO/g-C₃N₄ composite. The sporadic formed gC₃N₄ gems were found in the example along with rod and dumble like microstructures. The EDX range displayed in Fig. 3 shows the presence of C, N, Zn and O as fundamental components in the sample. The FESEM pictures of the ZnO blended at various aqueous temperatures are displayed in Fig. 3. At an aqueous temperature of 100°C, well defined bloom like ZnO with various sheets like subunit petals were shaped.

3.3. TEM/HR-TEM investigation

The TEM and HRTEM pictures of as-arranged ZnO and ZnO/gC₃N₄ composite are displayed in Fig. 3(a-d). The rod like morphology was again affirmed from the pictures. Further, the arrangement of interface among ZnO and g-C₃N₄ was obviously shown in Fig. 3(d). This is relied upon to lessen the electron-opening pair recombination rate fundamentally in the example contrasted with their singular analogs [23].

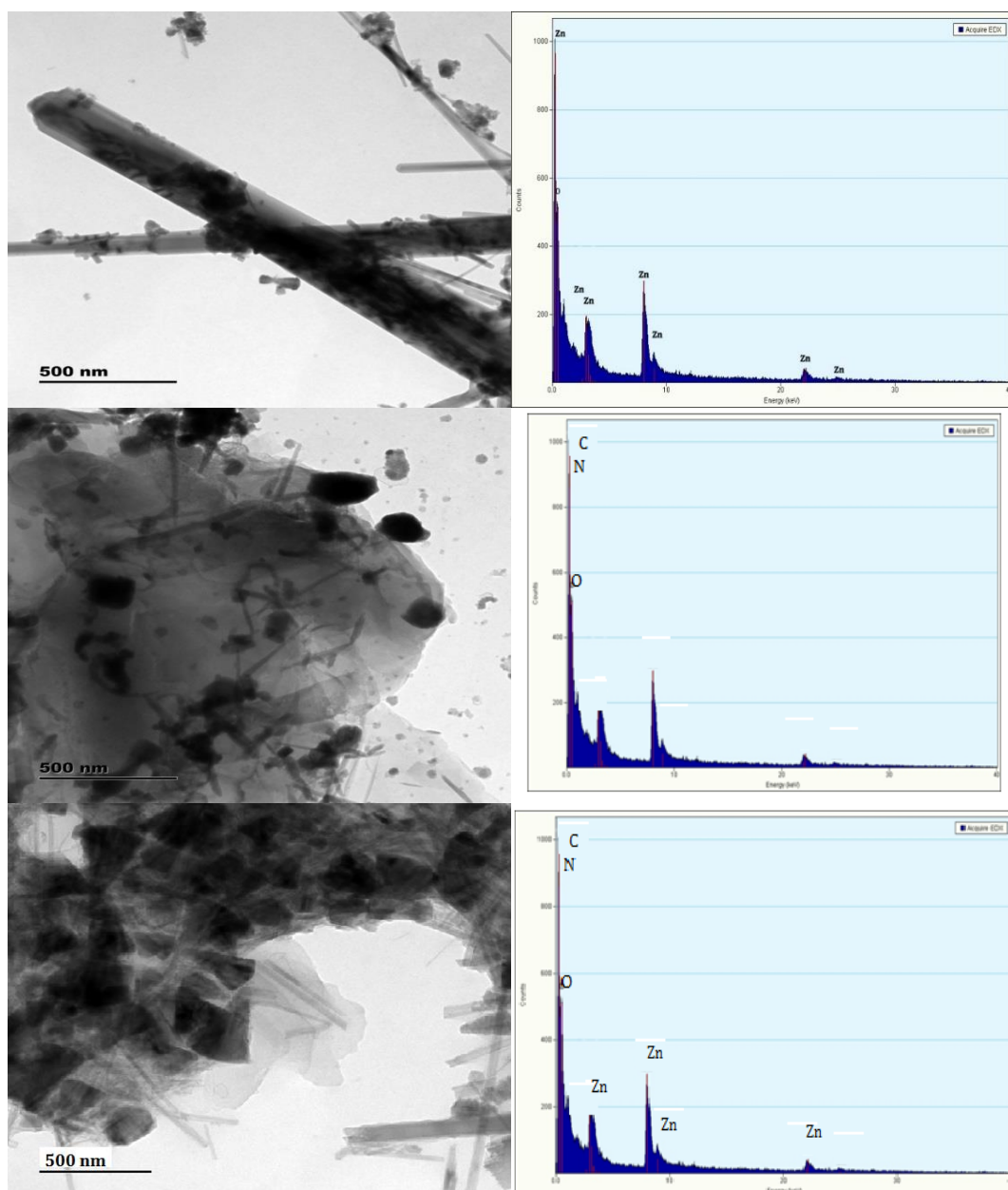


Fig. 3. TEM spectrum of (a) ZnO, (b) g-C₃N₄ and (c) g-C₃N₄@ZnO nanocomposites.

3.4. UV-Vis diffuse reflectance spectroscopy analysis

UV-Vis diffuse reflectance spectroscopy (DRS) was led to examine the impact of $g\text{-C}_3\text{N}_4$ on the optical properties of $g\text{-C}_3\text{N}_4@ZnO$ tests. The fuse of $g\text{-C}_3\text{N}_4$ into ZnO prompts a decline in the UV-vis reflectance (or the increment of the ingestion) over the whole frequency range. As introduced in Figure 4, the sharp key reflectance edge ascends at around 390 nm for the unadulterated ZnO nano rods, with basically no assimilation in the apparent light district which is steady with the way that ZnO NRs nearly can just utilize bright light [24] Compared to the unadulterated ZnO and $g\text{-C}_3\text{N}_4$, the $g\text{-C}_3\text{N}_4@ZnO$ stretches out the absorbance to the bright area as well as the noticeable locale, proposing that the recombination pace of the photograph prompted electron opening sets was effectively diminished in the heterostructured $g\text{-C}_3\text{N}_4@ZnO$ nanocomposite.

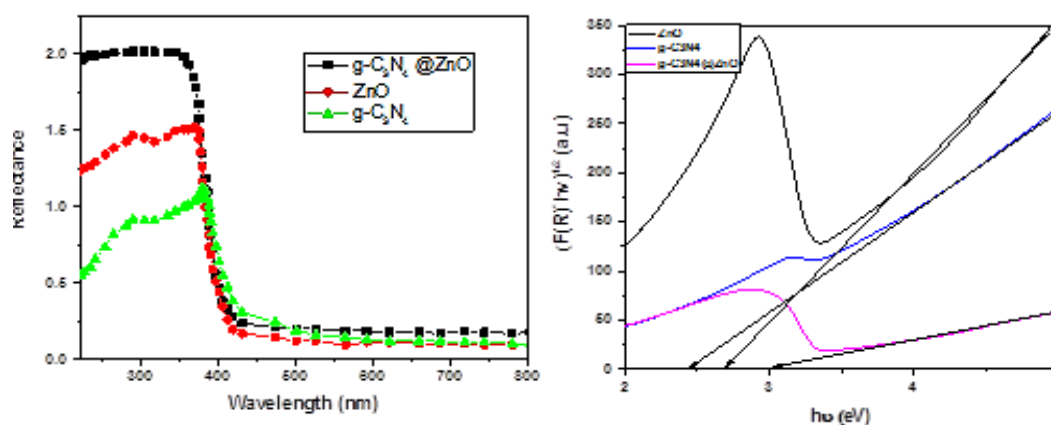


Fig. 4. (a) UV-Diffuse reflectance spectra (b) tauc plot of (a) ZnO, (b) $g\text{-C}_3\text{N}_4$ and (c) $g\text{-C}_3\text{N}_4@ZnO$ nanocomposites spectrum of (a) ZnO, (b) $g\text{-C}_3\text{N}_4$ and (c) $g\text{-C}_3\text{N}_4@ZnO$ NPs.

3.5. Dye removal pathways using photo catalysis

Figure 5(a) represents the ingestion spectra of the nitrophenol arrangement blended in with $g\text{-C}_3\text{N}_4@ZnO$ samples at various response times. It tends to be seen that $g\text{-C}_3\text{N}_4@ZnO$ sample is the retention top that lessens consistently with the illumination time, demonstrating that the nitrophenol fluid arrangement is disintegrated with the presence of the Z-7C sample under a semi daylight source. To evaluate the photocatalytic execution of the blended examples in the debasement response of the nitrophenol dye, the leftover convergence of nitrophenol dye is determined from the lingering force of the assimilation top at 601 nm.

Figure 5(b) shows the proportion between the remaining MB focus and the underlying nitrophenol dye fixation at various response times under apparent light utilizing distinctive photocatalytic-clear, unadulterated ZnO, $g\text{-C}_3\text{N}_4$, and $g\text{-C}_3\text{N}_4@ZnO$ samples, individually. All composite samples show great photocatalytic movement under the semi daylight. The photocatalytic exhibitions of clear, unadulterated ZnO, $g\text{-C}_3\text{N}_4$, and Z-1C, Z-3C, Z-5C, and Z-7C samples are 4.4%, 24.4%, 82.2%, 65.8%, 92.3%, 93.0%, and 96.8%, separately. This outcome suggests that the hybridization helps increment the MB corruption under the light illumination and test Z-7C shows the most noteworthy photocatalytic productivity. The upgraded photocatalytic action potentially benefitted from the proficient photoinduced charge from ZnO to $g\text{-C}_3\text{N}_4$.

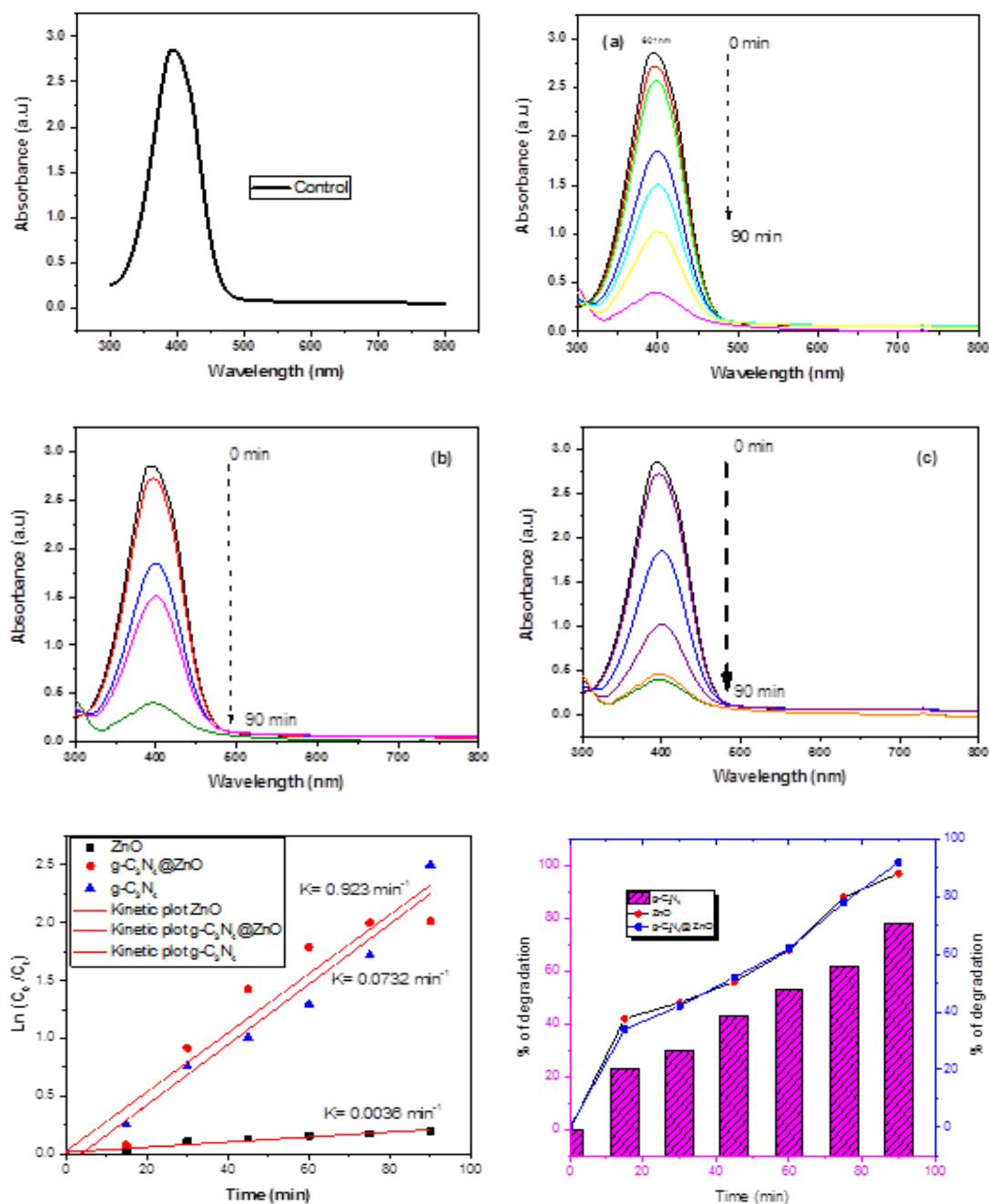


Fig. 5. UV Absorption spectrum of nitrophenol dye removal in different components like (a) ZnO, (b) g-C₃N₄ and (c) g-C₃N₄@ZnO nanocomposites at various time dependent with kinetic model and also percentage of dye removal process.

3.6. Photo catalysis Mechanism

The recombination of electrons and openings was controlled when TEOA was added to the framework as a forager to catch openings. Simultaneously, more electrons moved to the outer layer of the photocatalyst and responded with O₂ to frame ·O²⁻, which could upgrade the debasement of the MB under apparent light illumination by g-C₃N₄@ZnO. In this way, the really dynamic species are ·OH, ·O₂⁻, and h⁺ in the MB corruption process. The outcome is following the detailed outcomes [26-28].

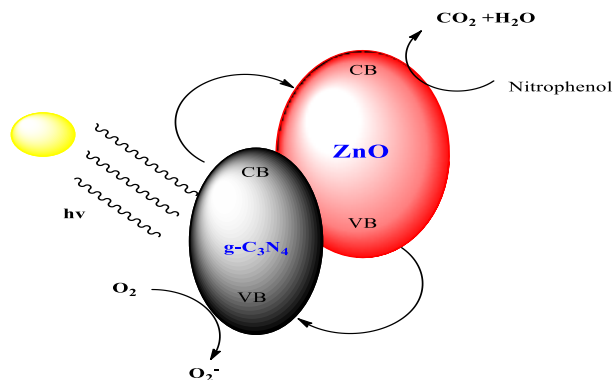


Fig. 6. Schematic diagram of photocatalytic dye removal mechanism.

4. Conclusion

In overview, a one-step hydrothermal method was employed the in situ heterostructure framework of g-C₃N₄@ZnO nanocomposites with varying g-C₃N₄ components. The forceful incorporation of g-C₃N₄ into nanocomposite results in a decline in crystallite, an increase in optical bandgap, and a modify in nanocomposite morphological features. In correlation to pure ZnO, g-C₃N₄ significantly improves the photocatalytic properties of g-C₃N₄@ZnO nanocomposites under visible light illumination. The nanostructure containing 7 wt.% g-C₃N₄ has the highest photocatalytic properties and is the most recyclable. The excellent photocatalytic effectiveness of the Z-7C nanocomposite was 0.923 min⁻¹, which is approximately 24.6 times that of pure ZnO (0.00036 min⁻¹). This improvement could be attributed to the g-C₃N₄@ZnO nanocomposite's broader and powerful assimilation of visible region optical band structure and greater absorbance, which are preferable for improving photocatalytic performance. Furthermore, the g-C₃N₄ lamellar structure allows photogenerated electrons transport to be faster transmitted, which is advantageous for direct photogenerated carrier transfer in heterostructure. These findings point to a suitable way for formulating an efficient photocatalyst that works under visible

References

- [1] N. B. Singh, G. Nagpal, S. Agrawal, Rachna, Environmental Technology & Innovation, vol. 11, pp. 187-240, 2018; <https://doi.org/10.1016/j.eti.2018.05.006>.
- [2] S.-M. Lam, J.-C. Sin, A. R. Mohamed, Materials Science in Semiconductor Processing, vol. 47, pp. 62-84, 2016; <https://doi.org/10.1016/j.mssp.2016.02.019>.
- [3] O. Sacco, D. Sannino, V. Vaiano, Applied Sciences, vol. 9, no. 3, pp. 472-486, 2019.
- Q. Pengpeng, P. Beomguk, C. Jongbok, T. Binota, P. B. Aniruddha, K. Jeehyeong, Ultrasonic Sonochemistry, vol. 45, pp. 29-49, 2018; <https://doi.org/10.3390/app9030472>.
- [4] K. Qi, B. Cheng, J. Yu, W. Ho, Journal of Alloys and Compounds, vol. 727, pp. 792-820, 2017; <https://doi.org/10.1016/j.jallcom.2017.08.142>.
- [5] V. L. Reddy Pullagurala, I. O. Adisa, S. Rawat et al., Environmental Pollution, vol. 241, pp. 1175-1181, 2018; <https://doi.org/10.1016/j.envpol.2018.06.036>.
- [6] K. Qi, B. Cheng, J. Yu, W. Ho, Journal of Alloys and Compounds, vol. 727, pp. 792-820, 2017 <https://doi.org/10.1016/j.jallcom.2017.08.142>.
- [7] V. Kumar, A. Dhiman, P. Sudhagar, and V. Krishnan, Applied Surface Science, vol. 447, pp. 802-815, 2018; <https://doi.org/10.1016/j.apsusc.2018.04.045>
- [8] M. Azarang, A. Shuhaimi, R. Yousefi, A. Moradi Golsheikh, M. Sookhikian, Ceramics International, vol. 40, no. 7, pp. 10217-10221, 2014; <https://doi.org/10.1016/j.ceramint.2014.02.109>

- [9] F. Hosseini, A. Kasaeian, F. Pourfayaz, M. Sheikhpour, D. Wen, *Materials Science in Semiconductor Processing*, vol. 83, pp. 175-185, 2018; <https://doi.org/10.1016/j.mssp.2018.04.042>.
- [10] E. Chubenko, I. Gerasimenko, V. Bondarenko, D. Zhigulin, *International Journal of Nanoscience*, vol. 18, pp. 1-4, 2019; <https://doi.org/10.1142/S0219581X19400453>.
- [11] R. Taziwa, L. Ntozakhe, M. Edson, *Journal of Nanoscience and Nanotechnology*, vol. 1, no. 13, pp. 1-8, 2017.
- [12] X. Wan, W. Ma, J. Yang et al., *The Journal of Alloys and Compounds*, vol. 737, pp. 197-206, 2018; <https://doi.org/10.1016/j.jallcom.2017.12.070>.
- [13] Z. Youssef, L. Colombeau, N. Yesmurzayeva et al., *Dyes and Pigments*, vol. 159, pp. 49-71, 2018; <https://doi.org/10.1016/j.dyepig.2018.06.002>.
- [14] I. M. Sundaram, S. Kalimuthu, G. Ponniah, *Composites Communications*, vol. 5, pp. 64-71, 2017; <https://doi.org/10.1016/j.coco.2017.07.003>.
- [15] W.-K. Jo, N. Clament Sagaya Selvam, *Journal of Hazardous Materials*, vol. 299, pp. 462-470, 2015; <https://doi.org/10.1016/j.jhazmat.2015.07.042>.
- [16] Lan Anh Luu Thi, Mateus Manuel Neto, Thang Pham Van, Trung Nguyen Ngoc, Tuyet Mai Nguyen Thi, Xuan Sang Nguyen, Cong Tu Nguyen, *Advances in Materials Science and Engineering*, Volume 2021, Article ID 6651633; <https://doi.org/10.1155/2021/6651633>.
- [17] L. R. Zou, G. F. Huang, D. F. Li, J. H. Liu, A. L. Pan, W. Q. Huang, *RSC Adv.* 6 (2016), 86688-86694, <https://doi.org/10.1039/c6ra20514c>; <https://doi.org/10.1039/C6RA20514C>
- [18] S. Li, T. Liu, Y. Zhang, W. Zeng, F. Pan, X. Peng, *Mater. Lett.* 143 (2015) 12-15, <https://doi.org/10.1016/j.matlet.2014.12.053>.
- [19] X. Chen, B. Zhou, S. Yang, H. Wu, Y. Wu, L. Wu, J. Pan, X. Xiong, *RSC Adv.* 5 (2015) 68953-68963, <https://doi.org/10.1039/C5RA11801H>.
- [20] S.C. Yan, Z.S. Li, Z.G. Zou, *Langmuir* 25 (2009) 10397-10401, <https://doi.org/10.1021/la900923z>.
- [21] S. Prabhu, M. Pudukudy, S. Sohila, S. Harish, M. Navaneethan, D. Navaneethan, R. Ramesh, Y. Hayakawa, *Synthesis, Opt. Mater.* 79 (2018) 186-195, <https://doi.org/10.1016/j.optmat.2018.02.061>.
- [22] J.X. Sun, Y.P. Yuan, L.G. Qiu, X. Jiang, A.J. Xie, Y.H. Shen, J.F. Zhu, *Dalton Trans.* 41 (2012) 6756-6763, <https://doi.org/10.1039/c2dt12474b>.
- [23] S. Prabhu, M. Pudukudy, S. Harish, M. Navaneethan, S. Sohila, K. Murugesan, R. Ramesh, *Materials Science in Semiconductor Processing* 106 (2020) 104754, <https://doi.org/10.1016/j.mssp.2019.104754>
- [24] N. C. Tu, P. V. Thang, L. T. Lan Anh et al., *Ceramics International*, vol. 46, no. 7, pp. 8711-8718, 2020.
- [25] W. Liu, M. Wang, C. Xu, S. Chen, *Chemical Engineering Journal*, vol. 209, pp. 386-393, 2012; <https://doi.org/10.1016/j.cej.2012.08.033>.
- [26] B. Chai, J. Yan, G. Fan, G. Song, C. Wang, *Chinese Journal of Catalysis*, vol. 41, no. 1, pp. 170-179, 2020; [https://doi.org/10.1016/S1872-2067\(19\)63383-8](https://doi.org/10.1016/S1872-2067(19)63383-8)
- [27] L. Hu, J. Yan, C. Wang, B. Chai, J. Li, *Chinese Journal of Catalysis*, vol. 40, no. 3, pp. 458-469, 2019; [https://doi.org/10.1016/S1872-2067\(18\)63181-X](https://doi.org/10.1016/S1872-2067(18)63181-X).
- [28] A. I. Navarro-Aguilar, S. Obregón, D. Sanchez-Martinez, D. B. Hernández-Uresti, *Journal of Photochemistry and Photobiology A: Chemistry*, vol. 384, Article ID 112010, 2019 <https://doi.org/10.1016/j.jphotochem.2019.112010>.